PROCEEDINGS OF SCIENCE

Halo–independent bounds on the WIMP–nucleon couplings from direct detection and neutrino observations based on the non–relativistic effective theory

Sunghyun Kang,[a,b,*] **Arpan Kar,**[a,b] **and Stefano Scopel,**[a,b]

[a] *Center for Quantum Spacetime, Sogang University, Seoul 121-742, South Korea*
[b] *Department of Physics, Sogang University, Seoul 121-742, South Korea*

E-mail: francis735@naver.com, arpankarphys@gmail.com, scopel@sogang.ac.kr

We discuss about the halo–independent bounds on the WIMP–nucleon couplings of the non–relativistic effective Hamiltonian that drives the scattering process off nuclei of a WIMP of spin 1/2. We will show that for most of the couplings the degree of relaxation of the halo–independent bounds compared to those obtained by assuming the Standard Halo Model is with a few exceptions relatively moderate in the low and high WIMP mass regimes, where it can be as small as a factor of 2, while in the intermediate mass range (10 - 200 GeV) it can be as large as 1000. An exception to this general pattern, with more moderate values of the bound relaxation, is observed in the case of the spin–dependent type WIMP–proton couplings with no or small momentum suppression, for which WIMP capture in the Sun is strongly enhanced because it is driven by scattering events off Hydrogen, the most abundant target in the Sun. Within this class of operators the relaxation is particularly small for interactions that are driven by only the velocity–dependent term, for which the solar capture signal is enhanced because of the high speed of scattering WIMPs inside the strong gravitational field of the Sun.

38th International Cosmic Ray Conference (ICRC2023)
26 July - 3 August, 2023
Nagoya, Japan

*Speaker

1. Introduction

Weakly Interacting Massive Particles (WIMPs) are one of the most popular candidates of the Cold Dark Matter (CDM) that is believed to constitute around 25% of the density of the Universe. Their scattering process off unclear targets is an important physical process entering in both Direct Detection (DD) experiments, that observe the recoil energy of nuclei, and experiments measuring signals of neutrinos produced by WIMP annihilations inside celestial bodies such as the Earth or the Sun, where the WIMPs are captured through the same scattering process as DD.

In both classes of experiments two major uncertainties arise in the calculation of expected signals: the WIMP–nucleus interaction and the WIMP speed distribution. Indeed, specific assumptions are usually made on those two aspects to interpret WIMP–searching experimental results. In terms of the WIMP–nucleus interaction, the most common choices are either a spin–independent (SI) or a spin–dependent (SD) interaction. On the other hand, as for the speed distribution, analytic estimations and numerical models of Galaxy formation are compatible to a Maxwellian in the galactic halo rest frame indicated as the Standard Halo Model (SHM). As a consequence the default way to show the results of WIMP searches is based on providing upper bounds on the SI and SD WIMP–nucleus cross section from DD and signals from neutrinos under the assumption of a Maxwellian speed distribution.

Since the DD process is non–relativistic (NR), the WIMP–nucleon interaction can be parameterized with an effective Hamiltonian $\mathcal{H}$. Such Hamiltonian for WIMPs of spin up to 1/2 has been systematically extended to the first order in the WIMP velocity $\vec{v}$ in Refs. [1, 2]:

$$\mathcal{H} = \sum_{\tau=0,1} \sum_{i=1}^{15} c_i^\tau O_i, \tag{1}$$

where the 14 Galilean–invariant operators O_i are listed in Table 1. With $\tau = 0{,}1$ the isospin, the c_i^τ's are the Wilson coefficients which can be arbitrary functions of the exchanged momentum q. In our analysis we will consider constant Wilson coefficients, which correspond to a contact interaction, and elastic scattering.

The isothermal Model provides a zero–order approximation describing the WIMP speed distribution. However, numerical simulations of Galaxy formation can only clarify statistical average properties of galactic halos and the growing number of observed dwarf galaxies hosted by the Milky Way suggests that our halo is not perfectly thermalized. Halo–independent approaches have been developed with the goal to avoid the dependence on the specific assumptions of the speed distribution.

Halo–independent techniques have been mainly developed in the context of direct detection. The most conservative bounds can be worked out with the only constraint:

$$\int_{u=0}^{\infty} f(u)du = 1, \tag{2}$$

for any arbitrary speed distribution $f(u)$.

In this kind of approach WIMP direct searches face a crucial limitation: due to a recoil energy threshold E_R^{th} all DD experiments have a speed threshold $u_{th}^{\rm DD}$ below which the sensitivity to the

$O_1 = 1_\chi 1_N$	$O_9 = i\vec{S}_\chi \cdot (\vec{S}_N \times \frac{\vec{q}}{m_N})$
$O_3 = i\vec{S}_N \cdot (\frac{\vec{q}}{m_N} \times \vec{v}^\perp)$	$O_{10} = i\vec{S}_N \cdot \frac{\vec{q}}{m_N}$
$O_4 = \vec{S}_\chi \cdot \vec{S}_N$	$O_{11} = i\vec{S}_\chi \cdot \frac{\vec{q}}{m_N}$
$O_5 = i\vec{S}_\chi \cdot (\frac{\vec{q}}{m_N} \times \vec{v}^\perp)$	$O_{12} = \vec{S}_\chi \cdot (\vec{S}_N \times \vec{v}^\perp)$
$O_6 = (\vec{S}_\chi \cdot \frac{\vec{q}}{m_N})(\vec{S}_N \cdot \frac{\vec{q}}{m_N})$	$O_{13} = i(\vec{S}_\chi \cdot \vec{v}^\perp)(\vec{S}_N \cdot \frac{\vec{q}}{m_N})$
$O_7 = \vec{S}_N \cdot \vec{v}^\perp$	$O_{14} = i(\vec{S}_\chi \cdot \frac{\vec{q}}{m_N})(\vec{S}_N \cdot \vec{v}^\perp)$
$O_8 = \vec{S}_\chi \cdot \vec{v}^\perp$	$O_{15} = -(\vec{S}_\chi \cdot \frac{\vec{q}}{m_N})((\vec{S}_N \times \vec{v}^\perp) \cdot \frac{\vec{q}}{m_N})$

Table 1: Non–relativistic Galilean invariant operators for a WIMP of spin 1/2 and up to linear terms in the WIMP velocity.

WIMP flux vanishes. As a consequence existing DD experiments can not probe the full range of WIMP speeds.

This problem can be solved by combining the constraints from DD with signals of neutrino telescopes (NTs) from WIMPs captured in the Sun. Such complementarity between DD and NT was exploited in Ref. [3] to develop a straightforward method independent on the $f(u)$ with the only constraint (2) and we will refer to this procedure as the "single stream method".

The applicability of the single–stream method of Ref. [3] is limited to the case of a single cross section or coupling. The O_i operators are the most general building blocks of the Hamiltonian (Eq. (1)) so that the WIMP–nucleus interaction driven by each of them is important in non–relativistic effective theory. As a consequence, we discuss the halo–independent single–stream bounds on c_i^p and c_i^n assuming such coupling is the only non–vanishing one in Eq. (1). We will analyze DD results from XENON1T, PICO–60 (C_3F_8) and PICO–60 (CF_3I) and NT results from IceCube and Super-Kamiokande.

2. Elastic WIMP–nucleus scattering in non–relativistic effective theory

The common quantity required for the calculation of the number of expected events for both the DD and NT signals is the differential cross section [1, 2]:

$$\frac{d\sigma_T}{dE_R} = \frac{2m_T}{4\pi u^2}\left[\frac{1}{2j_\chi + 1}\frac{1}{2j_T + 1}|\mathcal{M}_T|^2\right]. \tag{3}$$

2.1 Direct detection

From the differential cross section above, the total number of expected events in DD experiments is given by:

$$R_{\rm DD} = M\tau_{\rm exp}\left(\frac{\rho_\odot}{m_\chi}\right)\sum_T N_T \int du\, f(u)\, u \int_0^{E_R^{\rm max}} dE_R\, \zeta_T(E_R, E_1', E_2')\,\frac{d\sigma_T}{dE_R}, \tag{4}$$

with $E_R^{\rm max} = 2\mu_{\chi T}^2 u^2/m_T$ and ζ_T indicates the experimental response, while M is the fiducial mass and $\tau_{\rm exp}$ the live–time of data taking. Although DD experiments analyze their result in the Earth reference frame, since we are considering only the time–average of the rate, averaging away the effect of the Earth rotation around the Sun we can express equations in the reference frame of the Sun. Details of experiments used in this analysis are provided in [4].

2.2 Capture in the Sun

Assuming equilibrium between WIMP capture and annihilation ($\Gamma_\odot = C_\odot/2$), the neutrino flux measured by NT is given by:

$$\begin{aligned} C_\odot &= \left(\frac{\rho_\odot}{m_\chi}\right) \int du\, f(u)\, \frac{1}{u} \int_0^{R_\odot} dr\, 4\pi r^2\, w^2 \\ &\times \sum_T \rho_T(r)\, \Theta(u_T^{\text{C-max}} - u) \int_{m_\chi u^2/2}^{2\mu_{\chi T}^2 (u^2+v_{\text{esc}}^2)/m_T} dE_R\, \frac{d\sigma_T}{dE_R}, \end{aligned} \tag{5}$$

where $v_{\text{esc}}(r)$ is the escape speed at position r inside the Sun, $w^2 = u^2 + v_{\text{esc}}^2(r)$ the WIMP speed at the target position, and $u_T^{\text{C-max}} = v_{\text{esc}}(r)\sqrt{\frac{4m_\chi m_T}{(m_\chi - m_T)^2}}$ the maximum speed of a WIMP with mass m_χ for which capture through the interaction with a target T is possible. For the number density profile $\rho_T(r)$ of the different target nuclei in the Sun we use the Standard Solar Model AGSS09ph. The capture rate in Eq. (5) depends on the same speed distribution of DD.

3. Halo–independent constraints using the single stream method

Taking values as $u_{\text{esc}} = 560$ km/s and $v_\odot = 220$ km/s which imply $u_{\max} = 780$ km/s, Eqs. (4) and (5) can be written as:

$$R_{\text{DD}} = \int_0^{u_{\max}} du\, f(u)\, H_{\text{DD}}(u), \tag{6}$$

$$C_\odot = \int_0^{u_{\max}} du\, f(u)\, H_C(u), \tag{7}$$

Considering one effective coupling at a time, since $H(c_i^2, u)$ for both DD and NT is proportional to c_i^2, one can write $H(c_i^2, u) = c_i^2 H(c_i = 1, u)$, so that :

$$R(c_i^2) = \int_0^{u_{\max}} du\, f(u) \frac{c_i^2}{c_{i\,\max}^2(u)} H(c_{i\,\max}^2(u), u) = \int_0^{u_{\max}} du\, f(u) \frac{c_i^2}{c_{i\,\max}^2(u)} R_{\max} \le R_{\max}, \tag{8}$$

with:

$$H(c_{i\,\max}^2(u), u) = c_{i\,\max}^2(u) H(c_i = 1, u) = R_{\max}, \tag{9}$$

from which one obtains the following upper bound on the coupling c_i :

$$c_i^2 \le \left[\int_0^{u_{\max}} du \frac{f(u)}{c_{i\,\max}^2(u)}\right]^{-1}. \tag{10}$$

Considering one DD and NT bound, when c^{DD} and c^{NT} intersect at $\tilde{u}$ a unique halo–independent upper–limit is given by:

$$c^2 \leq 2\, c_*^2. \tag{11}$$

In above relations, $(c^{\mathrm{NT}})^2{}_{\mathrm{max}}(u)$ and $(c^{\mathrm{DD}})^2{}_{\mathrm{max}}(u)$ correspond to $c^2_{i\,\mathrm{max}}(u)$ for the NT and the DD experiments, respectively..

On the other hand, if the maximum coupling for DD is larger than c_* at $u = u_{\mathrm{max}}$ one has the bound:

$$c^2 \leq (c^{\mathrm{DD}})^2{}_{\mathrm{max}}(u_{\mathrm{max}}) + c_*^2, \tag{12}$$

while if the DD threshold exceeds u_{max}, in particular in the low m_χ region:

$$c^2 \leq (c^{\mathrm{NT}})^2\,(u_{\mathrm{max}})\,. \tag{13}$$

Note that the conditions above imply that in these cases the conservative upper bound on the effective coupling becomes sensitive to the choice of u_{max}. However, we checked that the effect of u_{max} is rather mild, reaching at most a factor $\lesssim 2$ at large m_χ for only some of the couplings. In our analysis, we repeated the procedure combining each DD bound with that of each NT one by one and took the most constraining limit.

4. Analysis

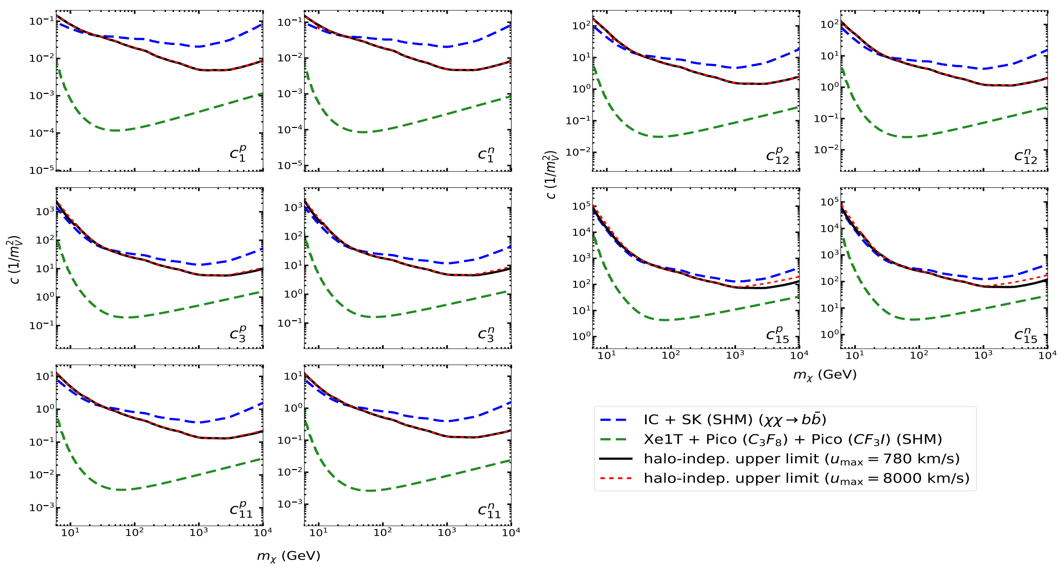

Figure 1: Halo–independent upper–limits on different non–relativistic effective couplings c_i's as a function of m_χ for both proton and neutron, assuming u_{max} = 780 km/s and 8000 km/s. In this figure the SI interactions have been considered.

NT experimental collaborations usually interpret their results assuming that the WIMP annihilates to W^+W^-, $\tau^+\tau^-$ or $b\bar{b}$. Among them we choose only annihilation to $b\bar{b}$, which yields the

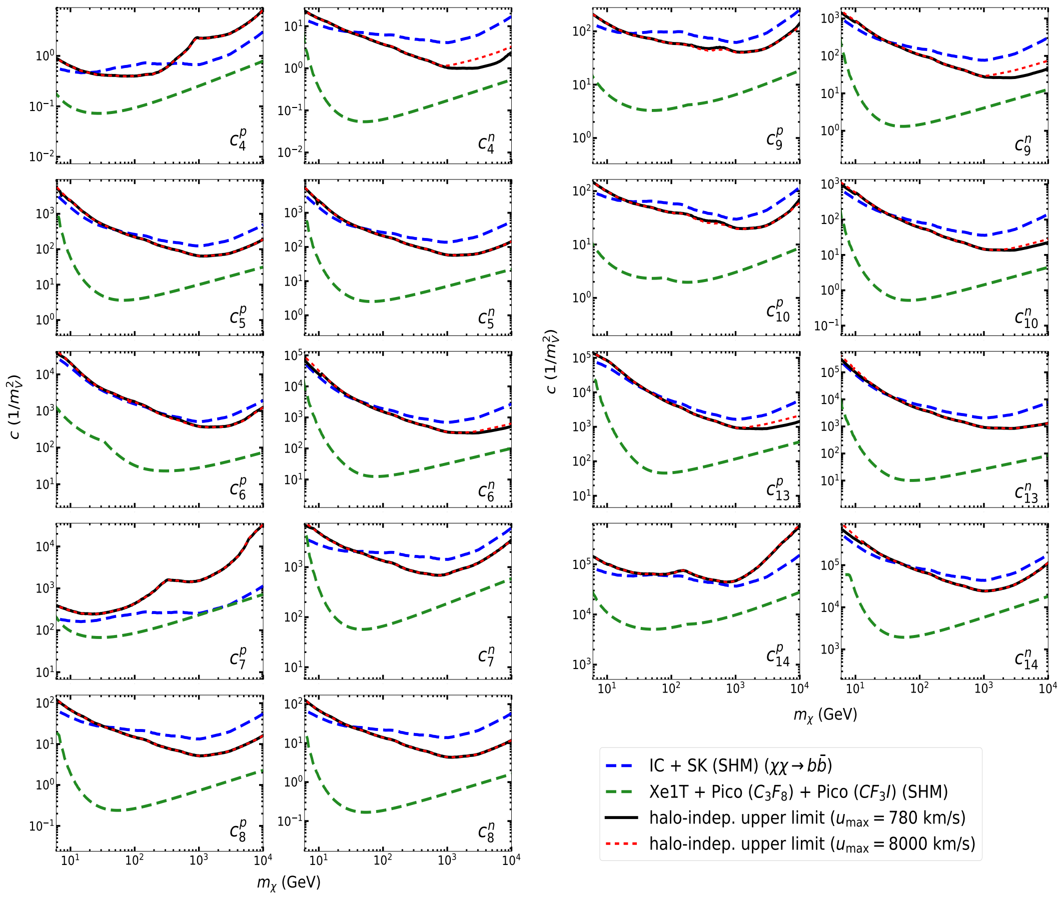

Figure 2: The same as Fig. 1, but considering the SD interactions.

most conservative bound. Further details about how we implement the neutrino and DD bounds are provided in the Appendix of [4].

The main results of our analysis are shown in Figs. 1 and 2. In these figures for each of the 14 operators listed in Table 1 the corresponding halo–independent conservative upper bounds on c^p and c^n are plotted as a function of the WIMP mass m_χ. In addition, the upper–limits on each coupling obtained from NT and DD experiments considering a Maxwellian $f_M(u)$ in the SHM are also shown. For $f_M(u)$ we assume a speed dispersion $u_{\rm rms}$ = 270 km/s, a Galactic escape speed $u_{\rm esc}$ = 560 km/s and we boost it in the solar frame assuming $v_\odot$ = 220 km/s. For the SHM case we plot at each WIMP mass the most constraining bounds from the NT and DD experiments.

In the two figures the effective operators are grouped in two main classes, SI and SD. In particular Fig. 1 refers to the operators O_1, O_3, O_{11}, O_{12} and O_{15} for which the WIMP–nucleus scattering process is driven by a SI–type interaction enhanced for heavy targets. The second class is SD operators, whose conservative bounds are shown in Fig. 2, corresponding to O_4, O_5, O_6, O_7, O_8, O_9, O_{10}, O_{13} and O_{14} requiring a non–vanishing nuclear spin.

To compare how the halo–independent approach can affect the bounds on different effective operators, in Fig. 3 we plot as a function of m_χ and for each of the couplings c_i^p and c_i^n a relaxing factor defined as the ratio between the following two quantities: the conservative exclusion plot and

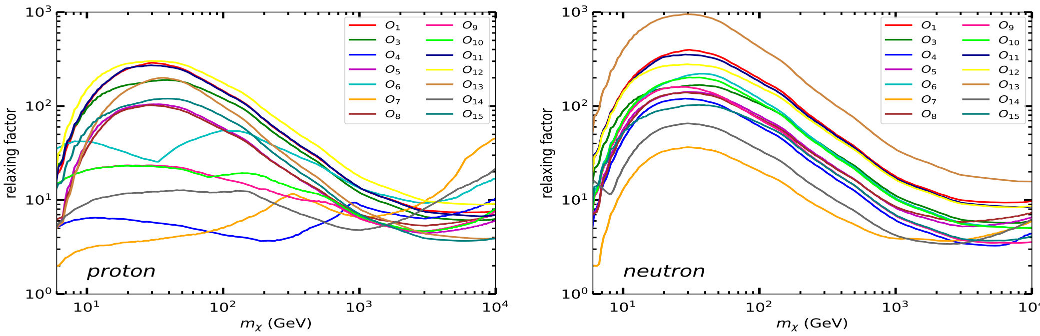

Figure 3: The relaxing factor is plotted for each operator O_i as a function of m_χ.

that obtained using for $f(u)$ a standard Maxwellian distribution $f_M(u)$.

In particular, the square of the relaxing factor r_f shown in Fig. 3 for a given coupling is explicitly given by:

$$r_f^2 = \frac{2c_*^2}{(c_{\rm SHM}^{\rm exp})^2} = 2c_*^2 \int_0^{u_{\rm max}} du \frac{f_M(u)}{(c^{\rm exp})^2_{\rm max}(u)} = 2c_*^2 \left\langle \frac{1}{(c^{\rm exp})^2_{\rm max}} \right\rangle \simeq 2c_*^2 \left\langle \frac{1}{(c^{\rm exp})^2_{\rm max}} \right\rangle_{\rm bulk}, \tag{14}$$

where "exp" indicates the NT or DD experiment that provides the strongest upper–limit on the coupling at a given m_χ in the case of a standard Maxwellian speed distribution f_M. The brackets $\langle \dots \rangle$ indicate an average weighted by the Maxwellian f_M while $\langle \dots \rangle_{\rm bulk}$ indicates the dominant contribution to the average from the bulk of the WIMP speeds, defined as:

$$\int_{\rm bulk} du f_M(u) \simeq 0.8. \tag{15}$$

The general features of the curves in Fig. 3 can be understood in terms of the speed dependence of the quantities $(c^{\rm DD})^2_{\rm max}(u)$ and $(c^{\rm NT})^2_{\rm max}(u)$ that enter Eq. (10). As shown in the left panel of Fig. 4, at small m_χ, $\tilde{u}$ is shifted to high speeds and the Maxwellian bulk is dominated by NT which is linearly increasing and not much different from c_* so that the relaxing factor is not large. On the other hand at large m_χ, as shown in right panel of Fig. 4, $\tilde{u}$ is moved to small speeds and the Maxwellian bulk is now dominated by DD. In this case $c^{\rm DD}_{max}$ is not much different from c_* which leads to moderate relaxing factor. However, in the intermediate mass range (10 - 200 GeV), there is a steep dependence on u inside the bulk of the Maxwellian, as shown in the middle panel of Fig. 4, so that the relaxing factor is large.

An exception to this pattern is represented by some of the WIMP–proton couplings namely O_4, O_7, O_9, O_{10}, O_{14}, and O_6 which are flattened in Fig. 3. In those cases WIMP capture is dominated by WIMP scattering off ^1H which is the most abundant target inside the Sun, bringing $c^{\rm NT}$ down in the small speed range. As a consequence the relaxing factor is reduced.

5. Conclusions

In the present work we have used the single–stream method introduced in Ref. [3] to obtain halo–independent bounds on each of the 28 WIMP–proton and WIMP–neutron couplings of the

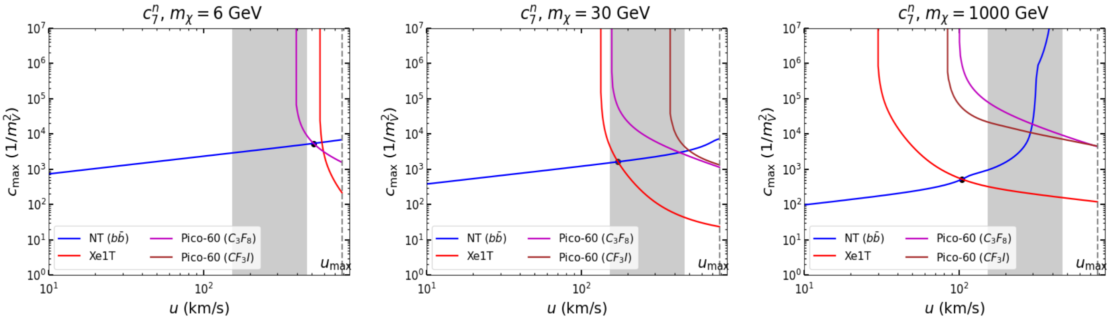

Figure 4: $c_{\rm max}$ corresponding to different experiments are shown as a function of u for three values of m_χ, i.e., 6 GeV (left), 30 GeV (middle) and 1000 GeV (right) to explain the general behavior of the relaxing factor at different WIMP masses (shown in Fig. 3). The grey shaded region indicates the speed range which corresponds to the bulk of the Maxwellian speed distribution.

effective non–relativistic Hamiltonian that drives the scattering process off nuclei of a WIMP of spin 1/2. The method only assumes that the speed distribution is normalized to one. In our analysis we have considered a single non–vanishing coupling at a time analyzing the results of three DD and two NT experiments.

Our main results are shown in Figs. 1 and 2, where the halo–independent conservative bound for each coupling is plotted as a function of the WIMP mass, and compared to the corresponding combined limit from direct detection and capture in the Sun in the case of a Standard Halo Model for which the WIMP speed distribution is assumed to be a Maxwellian. Introducing a relaxing factor to compare halo–independent bounds to those obtained by assuming SHM, we discussed its general properties. With few exceptions corresponding to couplings for which the capture rate is enhanced due to ^1H the relaxing factor is moderate at small and large WIMP masses, and large at intermediate masses.

References

[1] A. L. Fitzpatrick, W. Haxton, E. Katz, N. Lubbers and Y. Xu, *The effective field theory of dark matter direct detection*, Journal of Cosmology and Astroparticle Physics **2013** (feb, 2013) 004–004.

[2] N. Anand, A. L. Fitzpatrick and W. C. Haxton, *Weakly interacting massive particle-nucleus elastic scattering response*, Phys. Rev. C **89** (Jun, 2014) 065501.

[3] F. Ferrer, A. Ibarra and S. Wild, *A novel approach to derive halo-independent limits on dark matter properties*, JCAP **09** (2015) 052, [1506.03386].

[4] Sunghyun Kang and Arpan Kar and Stefano Scopel, *Halo-independent bounds on the non-relativistic effective theory of WIMP-nucleon scattering from direct detection and neutrino observations*, Journal of Cosmology and Astroparticle Physics**03** (2023) 011,[2212.05774].